RSC Advances

PAPER

View Article Online
View Journal | View Issue



Cite this: *RSC Adv.*, 2022, **12**, 28519

# A disulphide bond-mediated hetero-dimer of a hemoprotein and a fluorescent protein exhibiting efficient energy transfer†

Julian Wong Soon, Koji Oohora * and Takashi Hayashi *

Artificial protein hetero-dimerization is one of the promising strategies to construct protein-based chemical tools. In this work, cytochrome $b_{562}$, an electron transfer hemoprotein, and green fluorescent protein (GFP) mutants with cysteine residues added to their surfaces were conjugated *via* a pyridyl disulphide-based thiol–disulfide exchange reaction. The eight hetero-dimers, which have cysteine residues at different positions to form the disulphide bonds, were obtained and characterized by gel-electrophoresis, mass spectrometry and size exclusion chromatography. The fluorescence properties of the hetero-dimers were evaluated by fluorescence spectroscopy and fluorescence lifetime measurements. Efficient photoinduced energy transfer from the GFP chromophore to the heme cofactor was observed in each of the hetero-dimers. The energy transfer efficiency is strongly dependent on the cross-linking residues, reaching 96%. Furthermore, the estimated Förster distance and the structure-based maximum possible distances of the donor and acceptor suggest that one of the hetero-dimers has a rigid protein–protein structure with favourable properties for energy transfer. The disulphide bond-mediated protein hetero-dimerization is useful for screening functional protein systems towards further developments.

Received 21st August 2022
Accepted 22nd September 2022

DOI: 10.1039/d2ra05249k

rsc.li/rsc-advances



## Introduction

Proteins in their functional forms frequently exist as dimers and higher-order oligomers.[1] To gain insights into and develop bio-inspired applications based on these natural complex structures, artificial protein assemblies have been prepared by various approaches utilizing protein–protein interactions formed by metal coordination, covalent-linking, and non-covalent interactions among others.[2] Such known applications include drug delivery,[3] catalysis,[4] and biosensors.[5] Among the strategies used, site-specific disulphide bond formation has been reported for covalent linkage of supramolecular protein assemblies in protein crystals[6] and a metal coordinated unique cryptand structure.[7] Additionally, a disulphide bond cross-linkage is now commonly used in polymerization by dynamic covalent bonds.[8] The use of the disulphide bond as the linkage structure provides stability,[9] reversibility,[10] and stimuli responsiveness[11] in dynamic smart materials. Although the disulphide linkage can be formed spontaneously under aerobic conditions,[12] this type of random air-oxidation reaction can lead to mixed disulphide aggregations.[13] It tends to be a very slow reaction *in vivo* and is catalysed by protein disulphide isomerase,[14] thus leading to the employment of alternative catalysts and various oxidation methods in synthetic routes.[15] Due to these complications, we employ a pyridyl disulphide moiety which is known for its high selectivity and reactivity towards thiol groups to form a new disulphide bond.[16] The pyridyl disulphide group will activate a thiol group on one protein which will selectively react with a free thiol group on another protein to form a disulphide linkage.[17] However, protein hetero-dimerization using the pyridyl disulphide active species is quite limited.[18]

Herein, we employ green fluorescent protein (GFP) and cytochrome $b_{562}$ (Cyt $b_{562}$) (Fig. 1) for disulphide hetero-dimerization. Cyt $b_{562}$ is a small electron transfer protein containing a non-covalently bound heme as a co-factor. Previous reports[19] have used Cyt $b_{562}$ and a GFP mutant to construct a chimera *via* a conventional recombinant protein fusion method leading to bio-inspired tools.[20] Nagamune and co-workers utilized a Gly–Ser linker to prepare a fusion protein displaying 65% of energy transfer from the GFP mutant towards heme, while Jones and co-workers inserted Cyt $b_{562}$ into the GFP sequence to prepare a di-domain protein scaffold demonstrating the importance of inter-domain interactions in the energy transfer process. Although these previous efforts were successful in expression of the fusion protein, conjugation sites of the components were limited, and optimization of an appropriate linker is necessary. In this work, disulphide bond-mediated hetero-dimerization of Cyt $b_{562}$ and GFP using the pyridyl disulphide moiety is demonstrated and the energy

*Department of Applied Chemistry, Graduate School of Engineering, Osaka University, Suita, 565-0871, Japan. E-mail: oohora@chem.eng.osaka-u.ac.jp; thayashi@chem.eng.osaka-u.ac.jp*

† Electronic supplementary information (ESI) available. See https://doi.org/10.1039/d2ra05249k

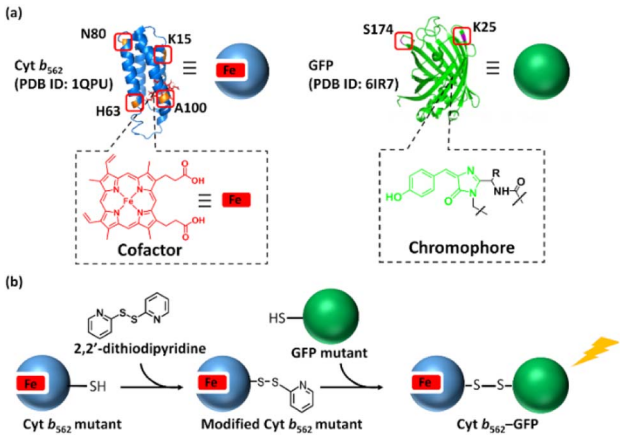


Scheme 1 (a) Mutation points of Cyt $b_{562}$ and GFP. (b) Schematic representation of the hetero-dimerization of Cyt $b_{562}$ and GFP mutants.

transfer efficiency in the Cyt $b_{562}$–GFP hetero-dimers is evaluated (Scheme 1).

## Experimental

### Preparation of modified Cyt $b_{562}$ mutants

Cyt $b_{562}$ mutants (500 μM, 900 μL) were reduced upon addition of a 1 M $DTT_{aq}$ (100 μL) solution and incubated for 1 h at 4 °C. DTT was removed using a HiTrap desalting column (eluent: 100 mM potassium phosphate buffer at pH 7.0) and the obtained protein solution was modified upon addition of 2,2′-dithiodipyridine (1 mM, 100 μL) in DMSO and incubated at 4 °C for 1 h. The modified protein was passed through a 5 mL HiTrap desalting column pre-equilibrated by 25 mL of 100 mM potassium phosphate buffer.

### Preparation and purification of hetero-dimer

Purified GFP mutants in 100 mM potassium phosphate buffer were reduced upon addition of 1 M $DTT_{aq}$ (100 μL) solution and incubated at 37 °C for 1 h before passing through HiTrap desalting column and diluted to 100 μM. Reduced GFP mutants were incubated with modified Cyt $b_{562}$ (3 eq.) at 25 °C for 2 h. The crude protein mixtures were purified straight away *via* Superdex 75 Increase 10/300 GL column using ÄKTA Purifier System (GE Healthcare) eluting by 100 mM potassium phosphate buffer containing 0.3 M NaCl at 0.5 mL $min^{-1}$ elution rate at 4 °C.

### Fluorescence lifetime analysis

Fluorescence lifetime measurements were measured at 25 °C in a constant temperature circulating water bath. The instrument response function (IRF) was determined from scattered light signals in the measurements of a LUDOX SM colloidal silica solution (30 wt% suspension in water, Sigma-Aldrich). The IRF showed a width of 60 ps measured as the full width at half maximum intensity. The IRF was employed in order to fit the fluorescence decay curves using a bi- or tri-exponential decay model. The quality of the fit was assessed from the $\chi^2$ values and distribution of the residuals with fixed $\tau$ values for the respective GFP mutants to achieve closest $\chi^2 = 1.00$ by bi- or tri-decay fitting. All fluorescence lifetime measurement values are an average of at least three sample measurements.

The intensity average lifetime, $\tau_{av}$, was calculated by eqn (1):

$$\tau = \frac{\sum_i A_i \tau_i}{\sum_i A_i} \quad (1)$$

where $A_i$ and $\tau_i$ represent the amplitude and the fluorescence lifetime respectively of the individual components.[21,22]

$$E = 1 - \frac{\tau}{\tau_{GFP}} \quad (2)$$

where $E$ is the energy transfer efficiency, $\tau_{GFP}$ value is lifetime obtained by the fluorescence decay for a corresponding GFP mutant, and $\tau_{av}$ is the average fluorescence lifetime calculated from eqn (1).

The averaged Förster distance ($R_0$), in which energy transfer from donor to acceptor occurs with a 50% probability, was calculated by eqn (3).[23]

$$R_0 = \left(\frac{9 \ln 10}{128\pi^5 N_A} \frac{\kappa^2 \phi_D}{n^4} J\right)^{1/6} \quad (3)$$

where $\kappa$ represents the orientation factor for the transition dipoles. Assuming that the dipole orientation factor ($\kappa^2$) was a limiting value ($\kappa^2$ is taken as 2/3 if the orientation of the donor and acceptor is assumed to be random), $n$ is the refractive index of water (1.333), $\phi_D$ is the quantum yield of GFP (0.68),[24] $J$ is the integral of the overlap of the emission from $GFP^{K25C}$ and the absorption from Cyt $b_{562}{}^{N80C}$ given by:

$$J = \int_0^\infty F_D(\lambda) E_A(\lambda) \lambda^4 dx \quad (4)$$

where $J$ was calculated using the experimental spectra giving $J = 5.67 \times 10^{14}$ $M^{-1}$ $cm^{-1}$ $nm^4$.[25]

The apparent distance ($r_{app}$) is estimated with the value of energy efficiency $E$ derived from time-resolved fluorescence measurement and eqn (5).

$$E = \frac{1}{1 + (r_{app}/R_0)^6} \quad (5)$$

### Distance estimation in protein structure

For the computational design of the modification of Cyt $b_{562}$ and GFP, the protein structural data of 1QPU and 6IR7 from the Protein Data Bank were utilized in PyMol, respectively. The distances between Cα and the heme centre of Cyt $b_{562}$ and between Cα and the fluorophore centre of GFP were estimated by the distance option in the measurement tool while highlighting the two specified residues (Cα to the heme centre of Cyt $b_{562}$ or GFP fluorophore).

## Results and discussion

Initially, the modification of a Cyt $b_{562}$ mutant having a cysteine residue at the N80 position located on the protein surface (Cyt

$b_{562}^{N80C}$) with 2,2′-dithiodipyridine was carried out. The modified Cyt $b_{562}^{N80C}$ bearing the pyridyl disulphide moiety was characterized by MALDI-TOF MS: found $m/z = 11\,880$, calcd $m/z = 11\,879$ (Fig. S1a†). The hetero-dimerization was first attempted using the wild-type GFP as it is known to have one exposed cysteine residue at the 47th position. The reactivity was first tested by conjugating the wild-type GFP ($GFP^{wt}$) with an excess amount of 2,2′-dithiodipyridine modified Cyt $b_{562}^{N80C}$. The analysis of the crude reaction mixture by non-reducing SDS-PAGE shows that $GFP^{wt}$ does not provide an efficient hetero-conjugation product with Cyt $b_{562}^{N80C}$ (Fig. 1a). Furthermore, an excess amount of homo-dimerization of Cyt $b_{562}^{N80C}$ was detected, although the band of the Cyt $b_{562}^{N80C}$ dimer overlaps with the $GFP^{wt}$ monomer band at *ca.* 30 kDa. This is plausibly caused by steric inaccessibility of the inherent cysteine residue at the 47th position.[26] Therefore, the exposed 25th position of GFP was selected as a conjugation site for the hetero-dimerization with Cyt $b_{562}^{N80C}$ after mutation of the 47th cysteine residue to alanine ($GFP^{K25C}$).[27] In comparison, $GFP^{K25C}$ readily conjugates to modified Cyt $b_{562}^{N80C}$ under the same conditions with high conjugation efficiency to afford the hetero-dimer (Cyt $b_{562}^{N80C}$–$GFP^{K25C}$) with 82% yield (Fig. 1b). Control experiments of air-oxidation of reduced Cyt $b_{562}^{N80C}$ and $GFP^{K25C}$ under the same conditions and analysed by non-reducing SDS-PAGE did not show hetero-dimerization product (Fig. S3†).

The crude Cyt $b_{562}^{N80C}$–$GFP^{K25C}$ mixtures purified using size exclusion chromatography (SEC, Fig. S2†) and ultrafiltration (30 kDa cut-off) showed a single distinct band at *ca.* 40 kDa in non-reducing SDS-PAGE consistent with the MALDI-TOF MS result: found $m/z = 38\,473$, calcd $m/z = 38\,472$ (Fig. 2a and b). In the SEC analyses, purified Cyt $b_{562}^{N80C}$–$GFP^{K25C}$ provides a single peak at 11.7 mL (Fig. 2c) which is a smaller elution volume compared to monomeric proteins of Cyt $b_{562}^{N80C}$ and $GFP^{K25C}$ eluted at 14.6 mL and 13.1 mL, respectively. These results indicate that the designed protein hetero-dimer can be successfully obtained with high purity. To verify the hetero-dimers linked by disulphide bonds, analysis by reducing SDS-PAGE with dithiothreitol (DTT) as a reductant was carried out.

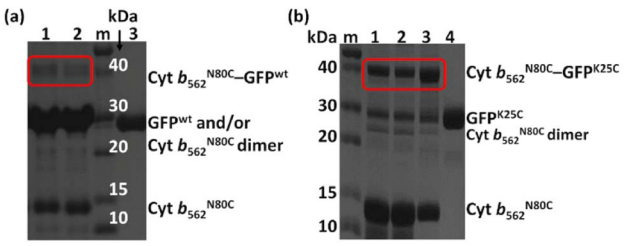


Fig. 1 (a) Non-reducing SDS-PAGE for samples in lanes 1 and 2 from $GFP^{wt}$ (100 μM) conjugation with an excess amount of pyridyl disulphide-modified Cyt $b_{562}^{N80C}$. Conditions: modified Cyt $b_{562}^{N80C}$: reduced $GFP^{wt} = 2:1$ in lane 1 and 3 : 1 in lane 2, and control $GFP^{wt}$ in lane 3. Lane m shows protein markers. (b) Non-reducing SDS-PAGE for samples in lanes 1, 2, and 3. Conditions: modified Cyt $b_{562}^{N80C}$: reduced $GFP^{K25C}$ 1 : 1 in lane 1, 2 : 1 in lane 2, 3 : 1 in lane 3, and $GFP^{K25C}$ control in lane 4. Lane m shows protein markers.

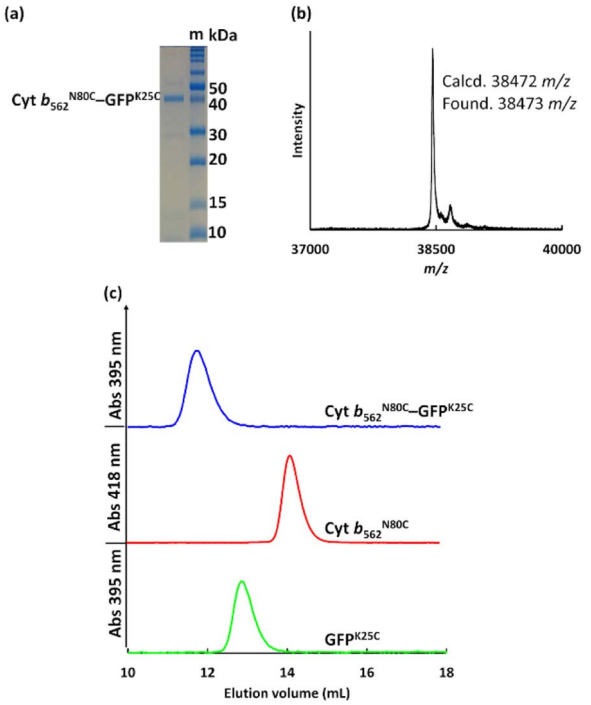


Fig. 2 (a) Non-reducing SDS-PAGE of purified Cyt $b_{562}^{N80C}$–$GFP^{K25C}$ with protein markers, m, (b) MALDI-TOF MS of Cyt $b_{562}^{N80C}$–$GFP^{K25C}$, and (c) SEC profiles of purified Cyt $b_{562}^{N80C}$–$GFP^{K25C}$, Cyt $b_{562}^{N80C}$, and $GFP^{K25C}$. Conditions: eluent = 100 mM potassium phosphate buffer containing 300 mM NaCl, pH 7.0 at 4 °C, column = Superdex 75 Increase 10/300 GL, elution rate = 0.5 mL $min^{-1}$.

The analysed samples indicate cleavage of the disulphide bond resulting in the separation of the two components, Cyt $b_{562}$ and GFP by the appearance of their monomeric bands at *ca.* 15 kDa and 30 kDa, respectively (Fig. S4†).

The apo form of modified Cyt $b_{562}$ was obtained by the conventional method[28] (Fig. S5†), and was subsequently conjugated with $GFP^{K25C}$. The reaction mixture was purified using the same method, and SEC analysis shows that apoCyt $b_{562}^{N80C}$–$GFP^{K25C}$ is generated with an elution volume similar to that of Cyt $b_{562}^{N80C}$–$GFP^{K25C}$ (Fig. S6†). The reconstitution of the apoCyt $b_{562}^{N80C}$–$GFP^{K25C}$ with heme illustrated in Fig. 3a results in the re-appearance of the characteristic Soret band absorption at 418 nm as shown in Fig. 3b, confirming successful heme binding. The fluorescence of the reconstituted hetero-dimer is *ca.* 90% quenched compared to apoCyt $b_{562}^{N80C}$–$GFP^{K25C}$ which exhibits fluorescence similar to that of $GFP^{K25C}$ (Fig. 3c). This indicates that the heme-dependent quenching occurs in the hetero-dimer. Moreover, the fluorescence lifetime measurements exhibit fast decay from both Cyt $b_{562}^{N80C}$–$GFP^{K25C}$ and the reconstituted hetero-dimer: $\tau_1 = 0.31$ ns and 0.28 ns, respectively (Fig. 4a and Table 1).[29,30] In contrast, apoCyt $b_{562}^{N80C}$–$GFP^{K25C}$ has $\tau = 2.93$ ns which is similar to that of $GFP^{K25C}$. The identical fluorescence lifetimes of $GFP^{K25C}$ and apoCyt $b_{562}^{N80C}$–$GFP^{K25C}$ indicate that there is no quenching behaviour within the apoCyt $b_{562}^{N80C}$–$GFP^{K25C}$ due to the absence of heme. Thus, the rapid decay observed in the

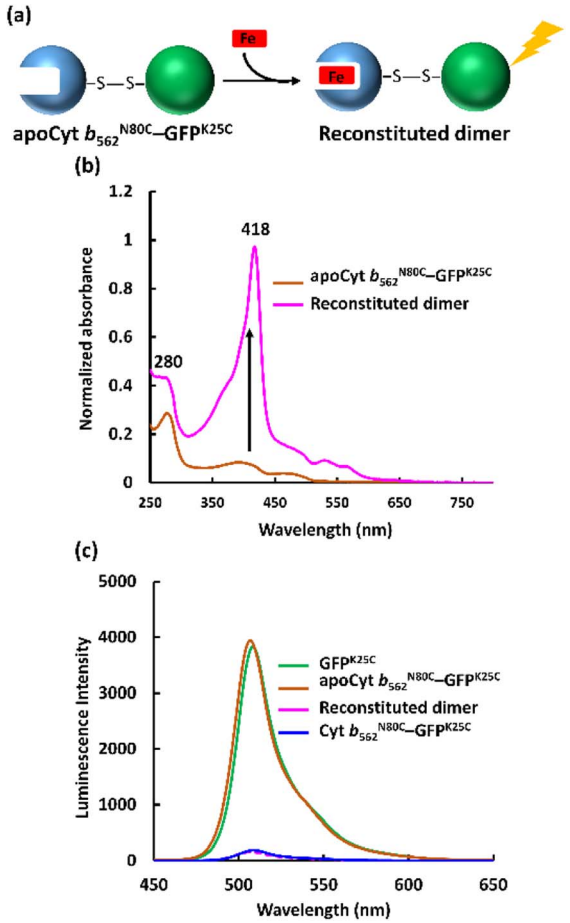


Fig. 3 (a) Schematic illustration of the hetero-dimer reconstitution with heme. (b) UV-vis spectra of apoCyt $b_{562}^{N80C}$–GFP$^{K25C}$ (brown) and reconstituted sample (pink). Conditions: [protein] = 50 μM in 100 mM potassium phosphate buffer, pH 7.0. (c) Fluorescence spectra of the hetero-dimers and GFP$^{K25C}$. Conditions: [protein] = 5 μM, in 100 mM potassium phosphate buffer, pH 7.0 at 25 °C, $\lambda_{ex}$ = 395 nm.

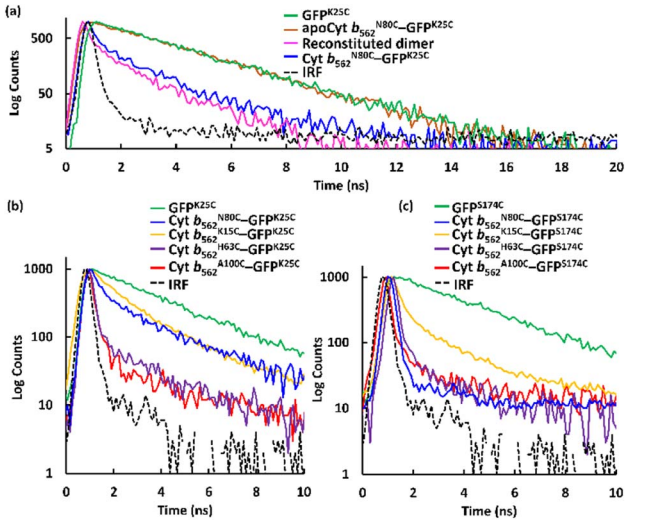


Fig. 4 Fluorescence lifetime measurements fitted taking the instrument response function (IRF) into account by a bi- or tri-exponential decay model for the respective samples. (a) GFP$^{K25C}$, apoCyt $b_{562}^{N80C}$–GFP$^{K25C}$, reconstituted dimer obtained by incorporation of heme into apoCyt $b_{562}^{N80C}$–GFP$^{K25C}$, and Cyt $b_{562}^{N80C}$–GFP$^{K25C}$. (b) GFP$^{K25C}$ and hetero-dimers with GFP$^{K25C}$. (c) GFP$^{S174C}$ and hetero-dimers with GFP$^{S174C}$. Conditions: [protein] = 20 μM, 1 mL, prepared in 0.1 M potassium phosphate buffer, pH 7.0 at 25 °C. Full scale fluorescence lifetime measurements are shown in Fig. S10.†

reconstituted dimer demonstrates efficient static quenching behaviour of the GFP$^{K25C}$ by the heme cofactor (Fig. 3c and 4a).

Three additional Cyt $b_{562}$ single mutants containing cysteine at positions K15 (Cyt $b_{562}^{K15C}$), H63 (Cyt $b_{562}^{H63C}$) and A100 (Cyt $b_{562}^{A100C}$) (Scheme 1a) and one GFP mutant containing cysteine at position S174 (GFP$^{S174C}$)[26] (Scheme 1a) were employed for the hetero-dimerization. The mutants were chosen due to their high expression levels, modification and hetero-conjugation yields. Similar to the Cyt $b_{562}^{N80C}$–GFP$^{K25C}$ hetero-dimerization, each Cyt $b_{562}$ mutant was modified with 2,2′-dithiodipyridine (Fig. S1†) and conjugated with GFP, yielding a total of seven purified hetero-dimers characterized by non-reducing SDS-PAGE (Fig. S7†) and MALDI-TOF MS (Fig. S8 and S9†).

Fig. 4b, c, and Table 1 show the results in the fluorescence lifetime measurements of a series of the hetero-dimers of Cyt $b_{562}$ and GFP mutants. Interestingly, different lifetime values were obtained and GFP$^{K25C}$ exhibits the shortest lifetime $\tau_1$ = 0.16 ns among the conjugations with Cyt $b_{562}^{A100C}$, while GFP$^{S174C}$ provides the shortest lifetime of $\tau_1$ = 0.10 ns among the conjugations with Cyt $b_{562}^{N80C}$.[29] The highest energy efficiencies obtained from Cyt $b_{562}^{A100C}$–GFP$^{K25C}$ and Cyt $b_{562}^{N80C}$–GFP$^{S174C}$, were calculated (eqn (2)) to be 89% and 96% respectively (Table 2).

Since the Cyt $b_{562}$ and GFP mutants have similar spectra to Cyt $b_{562}^{N80C}$ and GFP$^{K25C}$, respectively, superposition of the GFP$^{K25C}$ emission spectrum with the Cyt $b_{562}^{N80C}$ absorption spectrum shows overlap, suggesting the possible FRET of the hetero-dimer (Fig. S11c†). The Förster distance ($R_0$) was estimated to be 56 Å using the reported quantum yield of GFP,[24] assuming random donor and acceptor orientation.[29] From the calculated $R_0$ values and experimental results of energy transfer efficiencies ($E$), the apparent distances ($r_{app}$) between heme and GFP chromophore are found to be between 32 Å and 46 Å (Table 2). The distances from each cysteine mutation point to the chromophore or to the heme were estimated.[30] These estimations indicate that the distances between the Cα atom of the mutated residues and the heme centre in Cyt $b_{562}$ range from 9.6 Å to 23.9 Å, while in GFP the Cα atom of the K25 and S174 residues are situated away from the chromophore with a distance of 22.7 Å and 21.0 Å, respectively (Fig. S12 and S13†).[31] The maximum possible distances ($d_{max}$) between the chromophore and heme were also determined from these structural data and the typical length of the disulphide bond (2.04 Å),[32] showing that most hetero-dimers exhibit values similar to $r_{app}$ with differences of less than 7 Å (Table 2). The only exception is the Cyt $b_{562}^{N80C}$–GFP$^{S174C}$ hetero-dimer which exhibits a significantly shorter $r_{app}$ of 32 Å relative to $d_{max}$ of 49 Å. This result suggests a favourable conformation with a short distance and/or proper orientation of the heme cofactor and

Table 1 Fluorescence lifetime values of purified hetero-dimer[a]

| Protein | $\tau_1$ (ns) | $\tau_2$ (ns) | $\tau_3$ (ns) | $A_1$ ( %) | $A_2$ ( %) | $A_3$ ( %) | $\chi^2$ | $\tau_{av}$[b] (ns) |
|---|---|---|---|---|---|---|---|---|
| $GFP^{K25C}$ | 2.92 ± 0.06 | — | — | 100 | — | — | 1.05 ± 0.00 | |
| apoCyt $b_{562}{}^{N80C}$–$GFP^{K25C}$ | 2.93 ± 0.01 | | | 99.9 ± 0.05 | | | 1.00 ± 0.03 | |
| Reconstituted dimer[c] | 0.28 ± 0.08 | 2.92 | — | 93.7 ± 0.26 | 6.3 ± 0.16 | — | 0.99 ± 0.01 | |
| Cyt $b_{562}{}^{A100C}$–$GFP^{K25C}$ | 0.16 ± 0.04 | 1.35 ± 0.01 | 2.92 | 91.7 ± 0.05 | 4.90 ± 0.12 | 3.78 ± 0.52 | 1.09 ± 0.01 | 0.32 |
| Cyt $b_{562}{}^{H63C}$–$GFP^{K25C}$ | 0.20 ± 0.01 | 2.92 | —- | 93.7 ± 5.42 | 6.31 ± 5.42 | 6.31 ± 5.42 | 0.97 ± 0.00 | 0.37 |
| Cyt $b_{562}{}^{N80C}$–$GFP^{K25C}$ | 0.31 ± 0.03 | 1.53 ± 0.26 | 2.92 | 97.5 ± 0.79 | 2.50 ± 0.44 | —- | 1.07 ± 0.05 | 0.49 |
| Cyt $b_{562}{}^{K15C}$–$GFP^{K25C}$ | 0.56 ± 0.03 | 2.17 ± 0.33 | 2.92 | 92.9 ± 1.76 | 5.44 ± 0.88 | 1.68 ± 0.09 | 1.10 ± 0.07 | 0.70 |
| $GFP^{S174C}$ | 2.88 ± 0.02 | | | 100 | | | 1.02 ± 0.00 | |
| Cyt $b_{562}{}^{A100C}$–$GFP^{S174C}$ | 0.15 ± 0.00 | 2.88 | —- | 99.8 ± 0.01 | 0.22 ± 0.02 | —- | 1.06 ± 0.15 | 0.15 |
| Cyt $b_{562}{}^{H63C}$–$GFP^{S174C}$ | 0.12 ± 0.02 | 1.67 ± 0.10 | 2.88 | 89.8 ± 6.56 | 6.60 ± 4.25 | 3.59 ± 2.37 | 0.98 ± 0.12 | 0.32 |
| Cyt $b_{562}{}^{N80C}$–$GFP^{S174C}$ | 0.10 ± 0.00 | 0.75 ± 0.39 | 2.88 | 99.2 ± 0.07 | 0.77 ± 0.07 | —- | 1.06 ± 0.02 | 0.11 |
| Cyt $b_{562}{}^{K15C}$–$GFP^{S174C}$ | 0.23 ± 0.01 | 2.82 ± 0.05 | 2.88 | 80.5 ± 1.57 | 16.7 ± 1.50 | 2.76 ± 0.15 | 0.97 ± 0.02 | 0.74 |

[a] Conditions: [protein] = 20 μμM, 1 mL, prepared in 0.1 M potassium phosphate buffer pH 7.0 at 25 °C. Fluorescence lifetimes were evaluated by bi- or tri-exponential decay model. Values expressed are means ± S.D of three parallel measurements. [b] The intensity average lifetimes were calculated using eqn (1). [c] Hetero-dimer formed by apoCyt $b_{562}{}^{N80C}$–$GFP^{K25C}$ and then reconstituted by heme.

Table 2 Distances between acceptor and donor

| Protein | $E$ (%) | $d_h$[c] (Å) | $d_c$[d] (Å) | $d_{max}$[e] (Å) | $r_{app}$[f] (Å) |
|---|---|---|---|---|---|
| $GFP^{K25C}$ | | | 22.7 | | |
| Cyt $b_{562}{}^{A100C}$–$GFP^{K25C}$ | 89[a] | 9.6 | | 34.3 | 39 |
| Cyt $b_{562}{}^{H63C}$–$GFP^{K25C}$ | 87[a] | 12.0 | | 36.7 | 40 |
| Cyt $b_{562}{}^{N80C}$–$GFP^{K25C}$ | 83[a] | 23.9 | | 48.6 | 42 |
| Cyt $b_{562}{}^{K15C}$–$GFP^{K25C}$ | 76[a] | 15.4 | | 40.1 | 46 |
| $GFP^{S174C}$ | | | 21.0 | | |
| Cyt $b_{562}{}^{A100C}$–$GFP^{S174C}$ | 95[b] | 9.6 | | 34.3 | 34 |
| Cyt $b_{562}{}^{H63C}$–$GFP^{S174C}$ | 89[b] | 12.0 | | 36.7 | 39 |
| Cyt $b_{562}{}^{N80C}$–$GFP^{S174C}$ | 96[b] | 23.9 | | 48.6 | 32 |
| Cyt $b_{562}{}^{K15C}$–$GFP^{S174C}$ | 74[b] | 15.4 | | 40.1 | 46 |

[a] Energy efficiency for hetero-dimers conjugated with $GFP^{K25C}$ was calculated using eqn (2) and $\tau_1$ value of $GFP^{K25C}$. [b] Energy efficiency for hetero-dimers conjugated with $GFP^{S174C}$ was calculated using eqn (2) and $\tau_1$ value of $GFP^{S174C}$. [c] Distances from the Cα of the mutated residue in the crystal structure of wild type Cyt $b_{562}$ to the Fe center. [d] Distances from the Cα of the mutated residue in the crystal structure of wild type GFP to the GFP fluorophore. [e] The maximum possible distance was estimated as the sum of $d_h$ and $d_c$ with the typical length of the disulfide bond (2.04 Å).[32] [f] The apparent distances from heme to the GFP chromophore calculated using eqn (5), experimental $R_0$ and $E$.

chromophore in Cyt $b_{562}{}^{N80C}$–$GFP^{S174C}$. Although the single disulphide bond in the hetero-dimer is generally flexible with free rotation of the protein units, this finding indicates that a unique disulphide bond at appropriate mutation points triggers the induced protein–protein interaction[33] to strain the rotation achieving the favourable conformation for energy transfer.

## Conclusions

In conclusion, we successfully achieved hetero-dimerization of the Cyt $b_{562}$ and GFP mutants by employing a pyridyl disulphide moiety to rapidly react with thiols under mild conditions forming a disulphide bond. The purified hetero-dimers demonstrate efficient energy transfer in a heme-dependent quenching manner as foreseen. Simple protein linkage by disulphide bond formation is also useful to construct an interprotein energy transfer system as well as reported genetic protein fusion.[19] Our work presents a rapid and efficient site-selective bio-conjugation approach which allows for a much broader sampling and screening process to determine efficient energy transfer pairs. Further detailed investigations of the specific protein–protein interactions and hetero-dimer conformations are expected to contribute to the refinement of a useful process for hetero-dimerization of proteins.

## Conflicts of interest

There are no conflicts to declare.

## Acknowledgements

This research was funded by Grants-in-Aid for Scientific Research provided by JSPS KAKENHI Grant Numbers JP15H05804, JP18K19099, JP18KK0156, JP20H02755, JP20H00403 and JP20KK0315.

## Notes and references

1 (*a*) M. H. Ali and B. Imperiali, *Bioorg. Med. Chem.*, 2005, **13**, 5013–5020; (*b*) D. S. Goodsell and A. J. Olson, *Annu. Rev. Biophys. Biomol. Struct.*, 2000, **29**, 105–153.

2 (*a*) J. E. Padilla, C. Colovos and T. O. Yeates, *Proc. Natl. Acad. Sci. U. S. A.*, 2001, **98**, 2217–2221; (*b*) F. Sakai, G. Yang, M. S. Weiss, Y. Liu, G. Chen and M. Jiang, *Nat. Commun.*, 2014, **5**, 4634–4642; (*c*) S. Abe, B. Maity and T. Ueno, *Chem. Commun.*, 2016, **52**, 6496–6512; (*d*) Y. Suzuki, G. Cardone, D. Restrepo, P. D. Zavattieri, T. S. Baker and F. A. Tezcan, *Nature*, 2016, **533**, 369–373; (*e*) D. A. Uhlenheuer, D. Wasserberg, H. Nguyen, L. Zhang, C. Blum, V. Subramaniam and L. Brunsveld, *Chem.–Eur. J.*, 2009, **15**, 8779–8790.

3 (*a*) E. J. Lee, N. K. Lee and I. Kim, *Adv. Drug Delivery Rev.*, 2016, **106**, 157–171; (*b*) M. Zdanowicz and J. Chroboczek, *Acta Biochim. Pol.*, 2016, **63**, 469–473; (*c*) J. A. Mackay, M. Chen, J. R. McDaniel, W. G. Liu, A. J. Simnick and A. Chilkoti, *Nat. Mater.*, 2009, **8**, 993–999.

4 (*a*) W. Kang, J. Liu, J. Wang, Y. Nie, Z. Guo and J. Xia, *Bioconjugate Chem.*, 2014, **25**, 1387–1394; (*b*) T. Tong, S. Schoffelen, S. F. M. van Dongen, T. A. van Beek, H. Zuilhof and J. C. M. van Hest, *Chem. Sci.*, 2011, **2**, 1278–1285.

5 (*a*) J. Byeon, F. T. Llimpoco and R. C. Bailey, *Langmuir*, 2010, **26**, 15430–15435; (*b*) Y. Takaoka, A. Ojida and I. Hamachi, *Angew. Chem., Int. Ed.*, 2013, **52**, 4088–4106.

6 (*a*) S. Abe, T. T. Pham, H. Negishi, K. Yamashita, K. Hirata and T. Ueno, *Angew. Chem., Int. Ed.*, 2021, **60**, 12341–12345; (*b*) H. Negishi, S. Abe, K. Yamashita, K. Hirata, K. Niwase, M. Boudes, F. Coulibaly, H. Mori and T. Ueno, *Chem. Commun.*, 2018, **54**, 1988–1991; (*c*) T. K. Nguyen, H. Negishi, S. Abe and T. Ueno, *Chem. Sci.*, 2019, **10**, 1046–1051.

7 A. Medina-Morales, A. Perez, J. D. Brodin and F. A. Tezcan, *J. Am. Chem. Soc.*, 2013, **135**, 12013–12022.

8 (*a*) Q. Zhang, D. H. Qu, B. L. Feringa and H. Tian, *J. Am. Chem. Soc.*, 2022, **144**, 2022–2033; (*b*) A. H. J. Engwerda and S. P. Fletcher, *Nat. Commun.*, 2020, **11**, 4156–4163.

9 (*a*) J. Wang, L. Chen, J. Wu, W. Li, K. Liu, T. Masuda and A. Zhang, *Asian J. Chem.*, 2018, **13**, 3647–3652; (*b*) B. Li, J. Rozas and D. T. Haynie, *Biotechnol. Prog.*, 2006, **22**, 111–117.

10 (*a*) X. Lin, G. Godeau and M. W. Grinstaff, *New J. Chem.*, 2014, **38**, 5186–5189; (*b*) A. Fava, A. Iliceto and E. Camera, *J. Am. Chem. Soc.*, 1957, **79**, 833–838; (*c*) J. W. Sadownik and R. V. Ulijn, *Curr. Opin. Biotechnol.*, 2010, **21**, 401–411.

11 (*a*) Y. Z. You, C. Y. Hone and C. Y. Pan, *J. Phys. Chem. C*, 2007, **111**, 16161–16166; (*b*) O. Hayashida, K. Ichimura, D. Sato and T. Yasunaga, *J. Org. Chem.*, 2013, **78**, 5463–5469; (*c*) H. Wang, P. Wang, H. Xing, N. Li and X. Ji, *Polym. Chem.*, 2015, **53**, 2079–2084.

12 H. Nakamoto and J. C. A. Bardwell, *Biochim. Biophys. Acta*, 2004, **1694**, 111–119.

13 A. Zapun, J. C. A. Bardwell and T. E. Creighton, *Biochemistry*, 1993, **32**, 5083–5092.

14 (*a*) J. C. A. Bardwell and J. Beckwith, *Cell*, 1993, **74**, 769–771; (*b*) A. S. Patel and W. J. Lees, *Bioorg. Med. Chem.*, 2012, **20**, 1020–1028.

15 (*a*) T. Shi and D. L. Rabenstein, *Tetrahedron Lett.*, 2001, **42**, 7203–7206; (*b*) H. F. Gilbert, *J. Biol. Chem.*, 1997, **272**, 29399–29402; (*c*) J. D. Gough, R. H. Williams, A. E. Donofrio and W. J. Lees, *J. Am. Chem. Soc.*, 2002, **124**, 3885–3892; (*d*) T. E. Creighton and D. P. Goldenberg, *J. Mol. Biol.*, 1984, **179**, 497–526.

16 (*a*) J. D. Thomas and T. R. Burke, *Tetrahedron Lett.*, 2011, **52**, 4316–4319; (*b*) Y. Akiyama, Y. Nagasaki and K. Kataoka, *Bioconjugate Chem.*, 2004, **15**, 424–427; (*c*) D. R. Grassetti and J. F. Murray Jr, *Arch. Biochem. Biophys.*, 1967, **119**, 41–49.

17 (*a*) T. Ishii, M. Yamada, T. Hirase and Y. Nagasaki, *Polym. J.*, 2005, **37**, 221–228; (*b*) J. Xu, C. Boyer, V. Bulmus and T. P. Davis, *J. Polym. Sci., Polym. Chem.*, 2009, **47**, 4302–4313.

18 A. J. William, R. D. Ovadia and G. S. Giese, *Ind. Eng. Chem. Res.*, 2017, **56**, 1713–1722.

19 (*a*) S. Takeda, N. Kamiya, R. Arai and T. Nagamune, *Biochem. Biophys. Res. Commun.*, 2001, **289**, 299–304; (*b*) J. A. J. Arpino, H. Czapinska, A. Piasecka, W. R. Edwards, P. Barker, M. J. Gajda, M. Bochtler and D. D. Jones, *J. Am. Chem. Soc.*, 2012, **134**, 13632–13640.

20 (*a*) E. A. Dolgopolova, D. E. Williams, A. B. Greytak, A. M. Rice, M. D. Smith, J. A. Krause and N. B. Shustova, *Angew. Chem., Int. Ed.*, 2015, **54**, 13639–13643; (*b*) D. A. Hanna, R. M. Harvey, O. Martinez-Guzman, X. Yuan, B. Chandrasekharan, G. Raju, F. W. Outeen and A. R. Reddi, *Proc. Natl. Acad. Sci. U. S. A.*, 2016, **113**, 7539–7544; (*c*) S. Basak, N. Saikia, L. Dougherty, Z. Guo, F. Wu, F. Mindlin, J. W. Lary, J. L. Cole, F. Ding and M. E. Bowen, *J. Mol. Biol.*, 2021, **433**, 166793; (*d*) M. Sadoine, M. Reger, K. M. Wong and W. B. Frommer, *ACS Sens.*, 2021, **6**, 1779–1784; (*e*) N. Soleja, O. Manzoor, P. Nandal and M. Mohsin, *Org. Biomol. Chem.*, 2019, **17**, 2413–2422.

21 A. Sillen and Y. Engelborghs, *Photochem. Photobiol.*, 1998, **67**, 475–486.

22 S. E. Webber, *Photochem. Photobiol.*, 1997, **65**, 33–38.

23 W. R. Algar, N. Hildebrandt, S. S. Vogel and I. L. Medintz, *Nat. Methods*, 2019, **16**, 815–829.

24 R. Heim, A. B. Cubitt and R. Y. Tsien, *Nature*, 1995, **373**, 663–664.

25 M. J. Patel, G. Yilmaz, L. Bhatia, E. E. Biswas-Fiss and S. B. Biswas, *MethodsX*, 2018, **5**, 419–430.

26 L. M. Constantini, M. Baloban, M. L. Markwardt, M. A. Rizzo, F. Guo, V. V. Verkhusha and E. L. Snapp, *Nat. Commun.*, 2015, **6**, 7670–7683.

27 $GFP^{K25C}$ and $GFP^{S174C}$ contain cysteine residues at the 25th and 174th positions respectively, after mutating the inherent 47th cysteine to alanine.

28 F. W. J. Teale, *Biochim. Biophys. Acta*, 1959, **35**, 543.

29 J. R. Lakowicz, *Principles of Fluorescence Spectroscopy*, Springer, New York, 3rd edn, 2006.

30 The fluorescence decay of $GFP^{K25C}$ was fitted by a first-order exponential equation suggesting a single lifetime,[23] while a multi-exponential equation was used for the hetero-dimers due to more complex decays possibly showing characteristics of conformational heterogeneity (Table 1).

31 The distances from the Fe centre to C$\alpha$ of the mutated residue were estimated by the NMR structure of wild type Cyt $b_{562}$ (1QPU), while the distances from the chromophore centre to the $\alpha$ carbon of the mutated residue were estimated by the crystal structure of wild type GFP (6IR7).

32 M. Sun, Y. Wang, Q. Zhang, Y. Xia, W. Ge and D. Guo, *BMC Genomics*, 2017, **18**, 279–289.

33 K. Oohora, N. Fujimaki, R. Kajihara, H. Watanabe, T. Uchihashi and T. Hayashi, *J. Am. Chem. Soc.*, 2018, **140**, 10145–10148.